



OPEN ACCESS

EDITED BY

Roger Narayan,
University of North Carolina at Chapel Hill,
United States

REVIEWED BY

Shichao Bi,
Qingdao National Laboratory for Marine
Science and Technology, China
Viviana R. Lopes,
Uppsala University, Sweden

*CORRESPONDENCE

Hao Zhang,
✉ zhanghao57322@163.com
Mingming Liu,
✉ drliumingming@163.com
Yimeng Wang,
✉ doctor_wangym@163.com

[†]These authors have contributed equally
to this work

RECEIVED 06 June 2024

ACCEPTED 31 July 2024

PUBLISHED 09 August 2024

CITATION

Xie X, Feng X, Hong L, Yu X, Li H, Zhang H,
Liu M and Wang Y (2024) Evaluation of
antibacterial and osteogenic properties of a
novel Poly (acrylic acid)-calcium-zinc
biomineralized hydrogel.
Front. Mater. 11:1444750.
doi: 10.3389/fmats.2024.1444750

COPYRIGHT

© 2024 Xie, Feng, Hong, Yu, Li, Zhang, Liu and
Wang. This is an open-access article
distributed under the terms of the [Creative
Commons Attribution License \(CC BY\)](https://creativecommons.org/licenses/by/4.0/). The
use, distribution or reproduction in other
forums is permitted, provided the original
author(s) and the copyright owner(s) are
credited and that the original publication in
this journal is cited, in accordance with
accepted academic practice. No use,
distribution or reproduction is permitted
which does not comply with these terms.

Evaluation of antibacterial and osteogenic properties of a novel Poly (acrylic acid)-calcium-zinc biomineralized hydrogel

Xiaobin Xie^{1†}, Xiaoxiao Feng^{2†}, Lihui Hong^{2†}, Xinke Yu¹,
Hongye Li², Hao Zhang^{2*}, Mingming Liu^{2*} and Yimeng Wang^{1*}

¹Department of Orthopedics, The First Affiliated Hospital of Soochow University, Soochow University, Suzhou, China, ²Department of Orthopedic Surgery, The Second People's Hospital of Lianyungang, The Affiliated Lianyungang Clinical College of Jiangsu University, Lianyungang, China

Infectious bone defects are one of the thorny problems faced by orthopedists. Developing prosthetic materials with antimicrobial osteogenic features is a key solution. Biodegradable Polyacrylic acid (PAA)-based hydrogels have gained attention for their exceptional qualities. However, the influence of zinc ions on PAA-based mineralized hydrogels remains understudied. In this paper, Poly (acrylic acid)-calcium-zinc (PA-CZ) biomineralized hydrogel was prepared through ionic cross-linking and biomineralization. *In vitro* bacterial and cell tests demonstrated the hydrogel's exceptional biocompatibility, antibacterial, and osteogenic traits, along with good mechanical strength. The PA-CZ mineralized hydrogel lays the foundation for developing orthopedic implants with antimicrobial osteogenic features and offers a promising approach for treating infected bone defects.

KEYWORDS

antibacterial, osteogenesis, mineralized hydrogel, infectious bone defect, Polyacrylic acid

1 Introduction

Infection of the implant site remains a common and serious complication in orthopedic surgery. Infectious bone defects can cause delayed healing of damaged bones, which significantly increases treatment costs and may lead to amputation or patient death. It has a very high incidence rate and mortality and is a conundrum faced by orthopedists (Bhandari et al., 2015; Urish and Cassat, 2020). Infectious bone deformities are most commonly caused by *S. aureus* (*S. aureus*) (Kremers et al., 2015; Bakhshandeh et al., 2017; Urish and Cassat, 2020; Shen and Hu, 2021). Therefore, understanding the biological antibacterial characteristics of *S. aureus* is key to treating infectious bone defects. At present, surgical debridement, antibacterial treatment, and bone transplantation after eliminating infection are common methods for treating infectious bone defects (Cortés-Penfield and Kulkarni, 2019). Thorough clinical rehabilitation requires repeated surgical debridement, which increases the complexity of clinical interventions and the susceptibility of bone defects to infection. Antibiotics such as penicillin and cephalosporins are the main drugs used for treating infectious bone defects, but their bone tissue penetration is poor, and the drug's bone concentration reaches only 5%–20% of the serum concentration, leading to unstable antibacterial effects and prolonged treatment courses (Nandi et al., 2016). Additional drawbacks of long-term systemic antibiotic therapy include hazardous side

effects and drug resistance (Chee and Brown, 2020). Moreover, the development of related drug-carrying biomaterials is still limited by bacterial resistance to antibiotics.

These days, hydrogels are gaining a lot of interest because of their excellent delayed release, biodegradability, and biocompatibility (Naeem et al., 2024). Qin et al. (2023) reported that the addition of carboxymethyl chitosan (CMC) to methacrylated gelatin (GelMA) was effective in treating bone infections. However, the mechanical properties of GelMA as a matrix, which is susceptible to damage and deformation, remain inadequate. Therefore, developing novel hydrogel materials should have the following advantages: superior antibacterial properties, osteoinductive potential, biodegradability and stable mechanical properties.

Currently, inorganic materials with antibacterial effects include metallic materials such as silver (You et al., 2012; Pineda et al., 2022; Zhang et al., 2022), copper (Jing et al., 2008), zinc (Su et al., 2019; Vergara-Llanos et al., 2021) and titanium dioxide (Xu et al., 2018; Hu et al., 2023) and nonmetallic materials such as fluorine, fluoride (Nishida et al., 2021) and selenium (Manjunatha et al., 2021; Maqbool et al., 2021). The growth of bone tissue depends heavily on zinc. It contributes to the osteogenesis of the collagen matrix, which can influence osteoclast apoptosis and limit osteoclast development, in addition to its role in the composition of bone tissue (Molenda and Kolmas, 2023). In addition, in terms of antimicrobial properties, (Li et al., 2021) found that coating Hyaluronic acid (HA) samples with a high concentration of zinc ions significantly inhibited the growth of gram-negative anaerobic bacteria. It is thus clear that zinc has good antibacterial and osteoinductive properties. In an effort to obtain high-strength mechanical properties, biomineralization methods have been adopted to solve the problems associated with unstable and broken materials (Li et al., 2024). In a single step, Xu and colleagues created a mineralized hydrogel with high strength and toughness by copolymerizing acrylonitrile, 1-vinylimidazole, and polyethylene glycol diacrylate, followed by mineralization through *in situ* precipitation. Compared to the nonmineralized Polyvinyl alcohol (PAV) hydrogel, the mineralized hydrogel exhibited a two-fold uplift in tensile strength, a 5.5-fold growth in Young's modulus, and a 1.6-fold enhancement in compressive strength (Xu et al., 2017).

Currently, reported antibacterial materials containing zinc include zinc oxide, zinc gluconate, zinc peroxide and others (Nhu et al., 2022; Habib et al., 2023). However, the application of zinc ions in polyacrylate-based mineralized hydrogels has not yet been reported. In our preliminary experiments, we combined calcium and zinc ions with PAA and sodium metasilicate to synthesize mineralized hydrogels via ionic cross-linking and biomineralization. This biomineralized hydrogel can replicate the chemical composition and structural traits of natural bone by altering the mineralization duration. Furthermore, it has the potential to undergo functionalization through the binding of different inorganic metal ions. This study presents the synthesis of a mineralized hydrogel composed of PA-CZ and analyzes its physical and mechanical characteristics. The material's strong biocompatibility was validated, and its antibacterial and osteogenic induction capabilities were investigated. This research offers a novel perspective on creating effective antibacterial materials and addressing the treatment of infectious bone defects.

2 Methods

2.1 Materials

PAA was purchased from Thermo Fisher Scientific Company (USA). Sodium metasilicate and $\text{Ca}(\text{OH})_2$ were bought from Shanghai Aladdin Biochemical Technology Co., Ltd. CaCl_2 was obtained from Shanghai Yuanye Biotechnology Co., Ltd. ZnCl_2 was bought from Shanghai Macklin Biochemical Technology Co., Ltd.

2.2 Preparation of PA-CZ mineralized hydrogels

Sodium metasilicate anhydrous (0.25 g) was added to 10 mL of 3.125% PAA, and the mixture was stirred until completely dissolved and then ultrasonicated for 20 s to remove bubbles. During the stirring process, 2 mL of different concentrations of CaCl_2 and ZnCl_2 (PA-CZ₀ = 3 M CaCl_2 , PA-CZ₅₀ = 1.5 M CaCl_2 & 1.5 M ZnCl_2 , PA-CZ₇₅ = 0.75 M CaCl_2 & 2.25 M ZnCl_2 , PA-CZ₁₀₀ = 3 M ZnCl_2) were added to the solution and stirred for 15 min. Then, the hydrogel was immersed in deionized water for 24 h. Finally, the hydrogel was immersed in saturated $\text{Ca}(\text{OH})_2$ solution for 14 days to form a mineralized hydrogel.

2.3 Scanning electron microscopy (SEM)

The morphology of the mineralized hydrogels subjected to freeze-drying was analyzed using a scanning electron microscope (S-400 model, Hitachi, Japan). The hydrogel sample was fixed on the holder using conductive carbon tape. Then, a thin gold coating was evenly sputtered on the sample for 45 s using a plasma sputtering instrument, and the morphology was observed at 15 kV.

2.4 X-ray powder diffraction (XRD)

The mineralized hydrogel was freeze-dried and fully ground into powder. Next, the mineralized hydrogel powder was placed in the sample holder for analysis using XRD (D8 Advance, Germany) with a Cu target running at 40 mA and 40 kV. Data collection was performed within the 10°–80° range for 2 θ . A dwell time of 0.1 s and a scanning step of 0.02° were utilized in the process.

2.5 *In vitro* degradation test

The mineralized hydrogel that had been dried was placed in phosphate-buffered saline (PBS) for evaluation of its degradation in a laboratory setting. W_0 was used to denote the initial weight of the mineralized hydrogel. Subsequently, the samples were segregated into different sets and immersed in PBS before being kept at a constant temperature of 37°C in an incubator. The mineralized hydrogel was retrieved from the PBS solution on specific days including 1, 3, 5, 7, 10, 14, 21, 26, and 31. After that, it was dried at 37°C and weighed as W_t . The degradation pattern was determined utilizing the subsequent equation: Remaining rate (%) = $W_t/W_0 \times 100\%$.

2.6 Zinc ion release test

Mineralized hydrogels (0.2 g, PA-CZ₅₀, PA-CZ₇₅, and PA-CZ₁₀₀) were placed in 4 mL of PBS at room temperature. On days 1, 3, 5, 7, 10, 14, 20, 25, and 31, 10 μ L of PBS was removed, and the Zn²⁺ content was measured using a zinc ion detection kit (Nanjing Jiancheng Bioengineering Institute, China). Then, 10 μ L of PBS was added to maintain a constant volume of the solution. The zinc ion concentration was determined by analyzing the optical density (OD) value obtained at different time intervals.

2.7 Rheological properties

The hydrogels' rheological characteristics were assessed using a Discovery Hybrid Rheometer (HR2, TA Instrument, United States). An oscillatory strain sweep in dynamic mode was performed at room temperature, with an amplitude ranging from 0.1% to 100% and a frequency of 1 Hz.

2.8 Mechanical properties test

We employed a universal mechanical testing machine (Shanghai Hengyi, China) to assess the compressive strength of the mineralized hydrogels. The mineralized hydrogel was formed into cylinders (diameter: 6 mm, height: 12 mm). The compressive test was performed at room temperature with a compression speed of 5 mm/min.

2.9 Cytoskeleton staining

Mesenchymal stem cells from the bone marrow (BMSCs) of 8-week-old male Sprague-Dawley (SD) rats were harvested. The BMSCs was donated by Professor Li from Soochow University. Cultured at a density of 1×10^4 per well in Minimum Essential Medium α (α -MEM, Gibco, America) supplemented with 1% streptomycin-penicillin and 10% fetal bovine serum (FBS) for 24 h. Subsequently, the cells were treated with mineralized hydrogel extract (0.2 g/mL) for 3 days. After washing with PBS, the cells were fixed with 4% paraformaldehyde (PFA) (Biosharp, China) and incubated with immunostaining blocking solution (Beyotime, China) at 4°C overnight. The cytoskeleton was then stained using phalloidin (Abcam, United Kingdom) and 4',6-diamidino-2-phenylindole (DAPI) (Solarbio, China). Finally, images were captured and analyzed using a fluorescence microscope (Zeiss Axiovert 20).

2.10 Biocompatibility assessment

The biocompatibility of the mineralized hydrogels was examined using a Cell Counting Kit-8 (CCK-8) assay and live/dead staining methods. Initially, BMSCs were seeded into a 96-well plate at a concentration of 1×10^3 cells per well. Once cell attachment was complete, the medium was substituted with an extraction solution, and the cells were allowed to culture. Cell proliferation was assessed

after 1, 3, and 5 days using a CCK-8 cell proliferation detection kit from Beyotime, China. The absorbance was read at 450 nm through a microplate reader (BioTek, Winooski, VT, United States).

Separately, BMSCs were cultured in a 24-well plate at a density of 1×10^4 cells per well. Following cell adhesion, the medium was exchanged for the extract solution, and the cells were cultured for 3 days. Subsequently, a calcein AM/propidium iodide (PI) detection working solution (Solarbio, China) was added, and the cells were incubated in the dark at 37°C for 30 min. Post-incubation, the stained cells were observed under a fluorescence microscope.

2.11 *In vitro* antibacterial testing

The colony-forming unit (CFU) method was utilized to assess the antibacterial properties of the mineralized hydrogel against *S. aureus*. *S. aureus* was purchased from Ningbo Testobio Co. For the experiment, *S. aureus* was cultured with the mineralized hydrogel on a 24-well plate at a density of 5×10^4 CFU/well for a duration of 24 h. Subsequently, the bacterial mixture was uniformly spread onto a Luria-Bertani (LB) agar plate. The plate was then inverted and incubated at 37°C in a 5% CO₂ environment for 24 h. Following incubation, the colonies on the plate were counted and documented through photography.

2.12 Detection of bacterial biofilm inhibition

S. aureus suspension containing 5×10^7 colony-forming units per milliliter, LB medium, and sterile mineralized hydrogel were combined in 24-well plates and placed in a 37°C incubator for 48 h to develop bacterial biofilms. Then, 4% PFA was added to fix the *S. aureus*. Then, 1% crystal violet staining solution (Beyotime, China) was applied to stain the *S. aureus*, followed by decolorization with 95% ethanol solution. Finally, the absorbance at 595 nm was measured.

2.13 Alkaline phosphatase (ALP) staining

Mineralized hydrogel extracts were prepared using different hydrogel groups and osteogenic inductive medium (1% penicillin-streptomycin solution, 10% fetal bovine serum in α -MEM, 100 mmol/L β -glycerophosphate, 2 mmol/L ascorbic acid, and 1 μ mol/L dexamethasone) at a ratio of 0.2 g/mL. BMSCs were cultured with mineralized hydrogel extracts for 7 days. Next, fixed cells were treated with 4% PFA and stained using an ALP staining kit (Solarbio, China). Subsequently, the stained samples were visualized and captured under a microscope.

2.14 Alizarin red staining (ARS)

BMSCs were maintained in cultures containing mineralized hydrogel extracts for a duration of 14 days. At specific intervals, the cells were preserved using 4% PFA. Following this, ARS Kit (Solarbio, China) was employed to stain the calcium nodules. Lastly, the images were captured utilizing a microscope.

2.15 Statistical analysis

The statistical analysis employed one-way analysis of variance (ANOVA), and Tukey's multiple comparison test was utilized to assess group variances. Origin2021 was utilized for processing all data and images. Results are presented as mean \pm SD. A significance level of $*p < 0.05$ was deemed statistically significant.

3 Results

3.1 Synthesis and characterization of the PA-CZ mineralized hydrogels

The PA-CZ mineralized hydrogels were synthesized using PAA and bivalent cations (Ca^{2+} and Zn^{2+}). SEM was used to determine the internal morphology of the mineralized hydrogels with different Zn^{2+} concentrations. The internal cross section of the mineralized hydrogel possessed a porous structure. With increasing Zn^{2+} concentration, the porous structure became more condensed. Moreover, there were mineral deposits on the surface of the mineralized hydrogel after mineralization in a saturated $\text{Ca}(\text{OH})_2$ solution (Figure 1A). To determine the composition of the minerals, the mineralized hydrogels were analyzed using XRD (Figure 1B). No diffraction peaks were observed in the XRD results for the mineralized hydrogel, suggesting that the amorphous characteristics of the deposited minerals remained intact. To explore the stability of the mineralized material, an *in vitro* degradation test was performed in PBS. As shown in Figure 1C, the mineralized hydrogels cross-linked with pure Ca^{2+} degraded completely within 1 month. With increasing Zn^{2+} concentration, the degradation rate of the mineralized hydrogel decreased. The remaining masses of PA-CZ₂₅, PA-CZ₇₅, and PA-CZ₁₀₀ were $44.02\% \pm 3.91\%$, $49.31\% \pm 1.32\%$ and $62.19\% \pm 1.03\%$, respectively. Zn^{2+} ions possess good antibacterial properties. To evaluate the ability of the mineralized hydrogel to chelate Zn^{2+} , the release of Zn^{2+} from the PA-CZ mineralized hydrogels was measured using a zinc ion detection kit. The curve of Zn^{2+} release unfolded that the concentration of Zn^{2+} raised slowly and arrived a plateau at 25 days. The cumulative release of Zn^{2+} from PA-CZ₅₀, PA-CZ₇₅ and PA-CZ₁₀₀ on day 31 was 63.93 ± 11.40 , 92.63 ± 4.15 and 161.70 ± 5.09 $\mu\text{mol/L}$, respectively (Figure 1D). Finally, the mineralized hydrogel's mechanical properties were further investigated. Before mineralization, the PA-CZ hydrogel exhibited good shape. The dynamic storage modulus (G') and the loss modulus varied (G'') with angular frequency, indicating physical crosslinking of the hydrogels. The G' and G'' values were similar, indicating that the hydrogels were in a semiliquid state (Figure 1E). After mineralization, the compressive strength of the PA-CZ mineralized hydrogels improved significantly. According to the stress-strain curve and Young's modulus, the mineralized hydrogel chelated with pure Ca^{2+} had a greater compressive strength (7.51 ± 0.16 MPa, 187.98 ± 7.75 MPa) than Zn^{2+} . With increasing concentrations of Zn^{2+} chelated by the mineralized hydrogel, the compressive strength and Young's modulus decreased significantly (Figures 1F–H).

3.2 Evaluation of the biocompatibility of mineralized hydrogels

The morphology of the BMSCs was evaluated using cytoskeleton staining. It was revealed that the cells in all groups were well spread and did not exhibit obvious cytotoxicity (Figure 2A). BMSCs were cocultured with PA-CZ hydrogel extracts, and cell proliferation was detected with a CCK-8 kit. The results are shown in Figure 2B. When the cells were cocultured with the extracts of each group for 1 day, similar proliferation rates were observed. The cell proliferation in the PA-CZ₇₅ and PA-CZ₁₀₀ groups was significantly higher than that in the control group at 3 days, and the proliferation in all groups exceeded that of the control group at 5 days. The PA-CZ mineralized hydrogel, an antibacterial agent, promoted the proliferation of BMSCs and had good biocompatibility. Cell viability was evaluated using live-dead staining experiments (Figure 2C). Compared to the control group, the cells in the experimental group all survived, indicating that the BMSCs in each group were viable and maintained good proliferation throughout the culture period.

3.3 *In vitro* antibacterial evaluation

The antibacterial properties of the PA-CZ mineralized hydrogel were evaluated using *S. aureus*, a representative gram-positive bacterium. The results showed (Figure 3A) that the numbers of colonies in the PA-CZ₀ group and the ctrl group were similar. The number of colonies observed in the PA-CZ₁₀₀ group was significantly less than that in the ctrl group and PA-CZ₀ group, which indicated that PA-CZ₁₀₀ had high antibacterial activity against *S. aureus*. Quantitative analysis of the *S. aureus* colony count revealed that the antibacterial effect significantly improved with increasing zinc ion content, achieving an inhibition rate of up to approximately 90% (Figure 3C). In summary, zinc ions exhibit excellent antibacterial properties against *S. aureus*. The removal effect of the hydrogels on *S. aureus* biofilms was evaluated using crystal violet staining. The results showed (Figure 3B) that PA-CZ₁₀₀ had the greatest effect on biofilm removal. There was no significant difference between the PA-CZ₀ and ctrl groups, indicating that it had no clearing outcome on the biofilm. The colony photos showed trends consistent with the statistical results of crystal violet staining.

3.4 *In vitro* osteogenesis evaluation

The *in vitro* osteogenic activity of the PA-CZ mineralized hydrogel was investigated using ALP and ARS to assess the osteogenic differentiation of BMSCs. BMSCs were cocultured with PA-CZ hydrogel extracts for 7 days, after which the cells were stained with ALP. As shown in Figure 4A, compared with the control group, ALP expression was notably upregulated with the incorporation of calcium and zinc ions. After 14 days of culture, mineralized nodules were stained with Alizarin red and observed. Microscopy image analysis (Figure 4B) revealed that, compared with the control group, the addition of the PA-CZ hydrogel caused the BMSCs to produce more mineralized nodules, indicating that the PA-CZ hydrogel exhibited superior osteogenic induction ability.

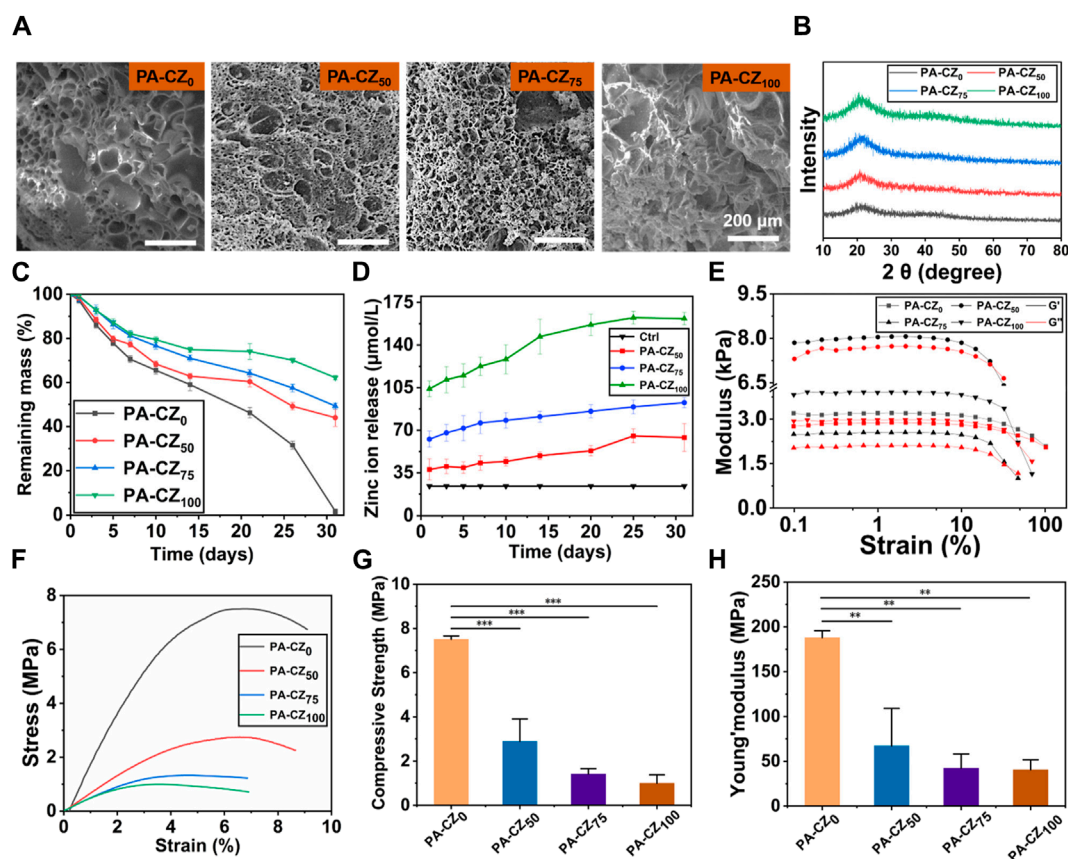


FIGURE 1

Characterization of the PA-CZ mineralized hydrogel. (A) SEM image of the mineralized hydrogel. (B) XRD image of the mineralized hydrogel. (C) Degradation test of mineralized hydrogel. (D) Zn^{2+} release test from mineralized hydrogels. (E) Plot of the rheological properties of the hydrogels. The mechanical properties of the PA-CZ mineralized hydrogel scaffolds included the stress-strain curve (F), compressive strength (G), and Young's modulus (H); * $p < 0.05$, ** $p < 0.01$, *** $p < 0.001$.

4 Discussion

As a polymer biomaterial, hydrogels can simulate the extracellular matrix and form a biomimetic local microenvironment, and they can also be used as a loading platform to construct various drug delivery systems. However, their inherent antibacterial and osteogenic abilities are limited, so relevant modifications or material loading are needed to enhance these properties (Cao et al., 2021). PAA is a nontoxic and degradable polymer that can obtain better chemical properties through chemical modification of carboxyl groups (Arkaban et al., 2022). Different configurations of PAA and nanostructures have demonstrated significant potential across numerous areas, including antibacterial applications, cancer treatment, biosensor technology, and tissue engineering (Arkaban et al., 2022). Wen et al. reported that PAA-based mineralized hydrogels can induce osteogenic differentiation, adjust to uneven hard tissue defects, and facilitate bone tissue regeneration (Wen et al., 2023). Zinc exhibits effective antibacterial properties against various bacterial strains and strikes a superior balance between its antibacterial efficacy and cytotoxicity compared to other antibacterial metals like silver and copper (Jin et al., 2014). Therefore, in this study, PAA and calcium zinc ions were used to prepare hydrogels through physical cross-linking.

The hydrogel itself has weak mechanical properties; therefore, mineralization was employed to increase its compressive strength and Young's modulus, thereby enhancing its mechanical properties (Figure 5A).

The management of bone defects caused by infections has consistently posed a significant challenge in the field of orthopedics. Its treatment consists of two key components: elimination of infection and restoration of bone defects. It is known that in the case of bacterial infection, the repair and healing of bone defects are extremely slow and may even worsen (Cui et al., 2022). At present, numerous materials exhibiting both antibacterial and osteogenic properties have been created in the field of tissue engineering. These materials integrate metal ions, pharmaceuticals, and biomaterials (Budiatin et al., 2021; Qiu et al., 2022; Xu et al., 2022). Qiu et al. explored the efficacy of using a scaffold made of β -tricalcium phosphate in conjunction with vancomycin hydrochloride incorporated into polylactic-co-glycolic acid microspheres for the purpose of treating bone defects that have become infected (Qiu et al., 2022). In this study, Zn^{2+} was continuously and stably released from the PA-CZ hydrogel. With increasing soaking time, the concentration of released zinc ions increased, reaching a highest cumulative concentration of $103.96 \pm 6.42 \mu\text{mol/L}$ after

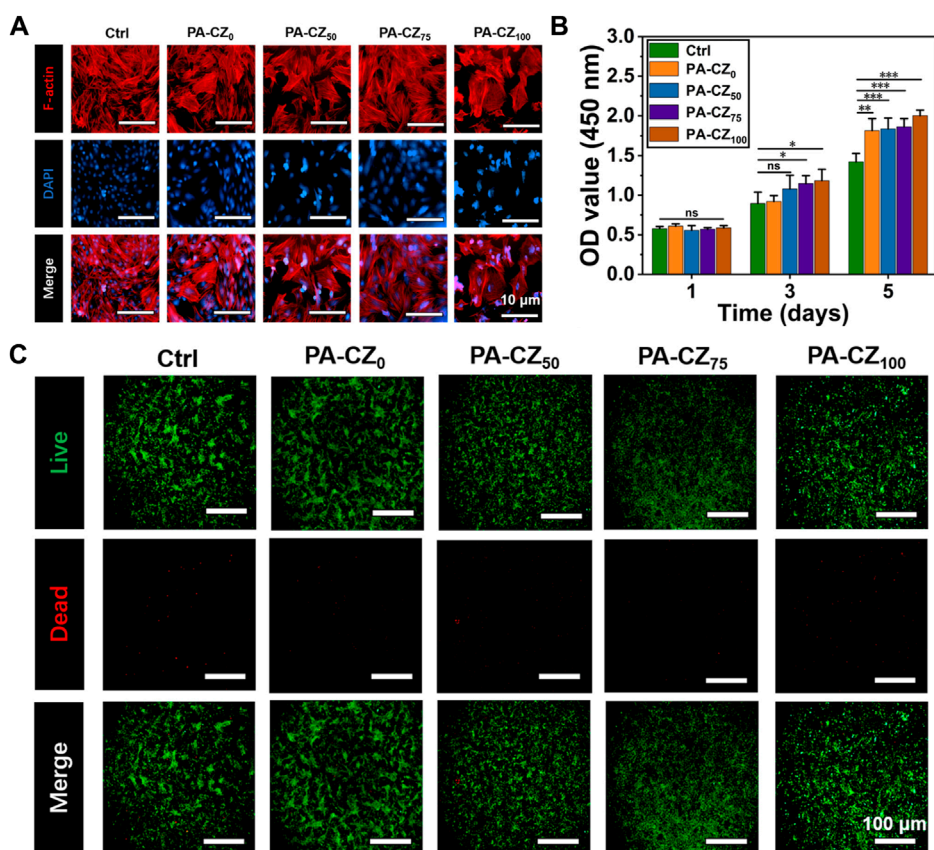


FIGURE 2 *In vitro* biocompatibility evaluation of the PA-CZ mineralized hydrogel. (A) Cytoskeletal staining of BMSCs. (B) The CCK-8 method was used to detect the proliferation of BMSCs on days 1, 3, and 5. (C) Fluorescence image of live-dead-stained BMSCs. * $p < 0.05$, ** $p < 0.01$, *** $p < 0.001$.

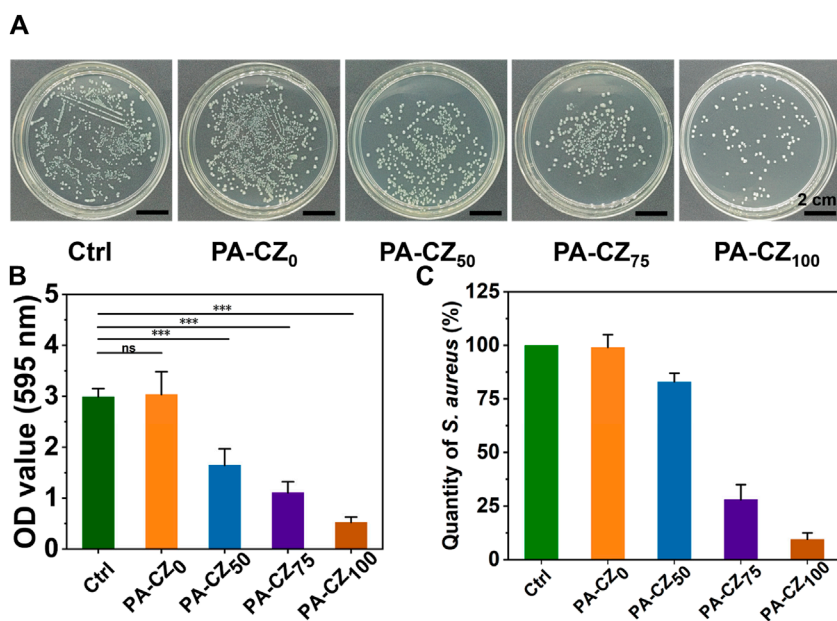


FIGURE 3 *In vitro* antibacterial performance evaluation of the PA-CZ mineralized hydrogel. (A) Photograph of *S. aureus* colonies cultured on LB agar plates. (B) Crystal violet staining was used to detect *S. aureus* biofilm formation. (C) Quantitative analysis of antibacterial rate. * $p < 0.05$, ** $p < 0.01$, *** $p < 0.001$.

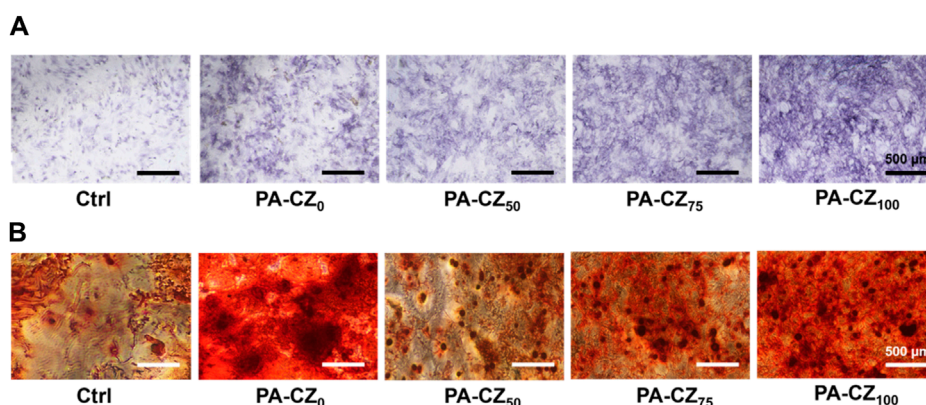


FIGURE 4

In vitro osteogenic induction ability of different PA-CZ mineralized hydrogels. (A) ALP staining image of BMSCs cultured in PA-CZ mineralized hydrogel extract for 7 days. (B) ARS image of BMSCs cultured in PA-CZ mineralized hydrogel extract for 14 days.

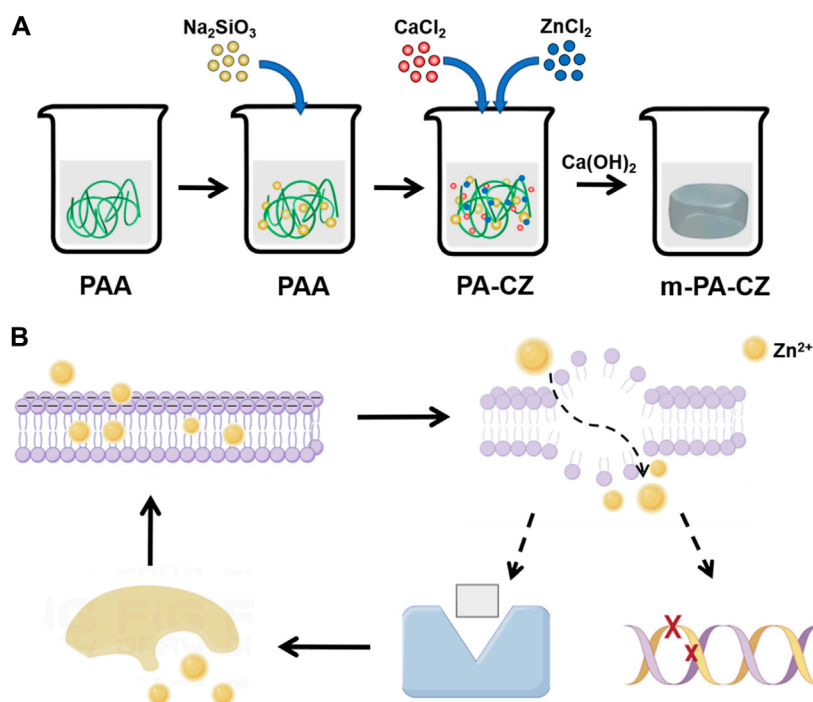


FIGURE 5

(A) PA-CZ mineralized hydrogel preparation process. (B) The antibacterial mechanism of Zn ions.

1 day (Figure 1D). Zinc is crucial for cellular proliferation and the induction of osteogenesis. Hence, it is especially vital to meticulously regulate zinc concentration and release, as elevated levels of zinc may lead to cytotoxic effects and potentially apoptosis (Yu et al., 2020). Zinc ions can attach to bacterial cell membranes, significantly enhancing their permeability and causing substantial cytoplasmic leakage (Feng et al., 2018). Bacterial death can also be induced by zinc ions through mechanisms such as protein inactivation, generation of substantial reactive oxygen species, and DNA damage, which subsequently impacts biofilm formation (Figure 5B) (Li et al., 2018; Yang et al., 2022). In this study, as the concentration of Zn^{2+}

increased, the count of *S. aureus* colonies was greatly reduced, the antibacterial rate reached 90% (Figure 3A), and the clearance rate of biofilms also significantly improved (Figure 3B). This indicates that zinc exhibits good antibacterial properties against *S. aureus*. Furthermore, it was found that Zn can induce osteogenic differentiation (Figure 4) and is nontoxic to BMSCs (Figure 2). In summary, the PA-CZ mineralized hydrogel exhibits superior biocompatibility, osteogenic properties, and antibacterial properties against *S. aureus*, and its use as an orthopedic implant represents an effective strategy to address the problem of *S. aureus*-infected bone defects.

5 Conclusion

In summary, a PA-CZ mineralized hydrogel with superior antibacterial properties against *S. aureus* and osteogenic properties was prepared through physical cross-linking and mineralization in this study. The osteogenic differentiation of BMSCs is induced via the deliver of zinc ions while inhibiting bacterial growth. However, research on PA-CZ mineralized hydrogels is still in the *in vitro* experimental stage, and *in vivo* research needs to be further improved to promote clinical translation and application. Moreover, the antibacterial characteristics of PA-CZ mineralized hydrogels against *S. aureus* still have significant potential for enhancement. The use of PA-CZ mineralized hydrogel, a material with dual antibacterial and osteogenic functions, represents an effective method for treating *S. aureus* infected bone defects. Whether it is material design or research on antibacterial mechanisms, they are subject to future research and exploration and have broad application prospects.

Data availability statement

The original contributions presented in the study are included in the article/supplementary material, further inquiries can be directed to the corresponding authors.

Ethics statement

Ethical review and approval was not required for the study as the cell lines used in the study have been gifted by Prof. Li of Soochow University.

Author contributions

XX: Conceptualization, Data curation, Formal Analysis, Writing–original draft. XF: Conceptualization, Data curation,

Formal Analysis, Writing–original draft. LH: Data curation, Formal Analysis, Writing–original draft. XY: Data curation, Formal Analysis, Writing–review and editing. HL: Data curation, Writing–review and editing. HZ: Funding acquisition, Investigation, Supervision, Writing–review and editing. ML: Conceptualization, Investigation, Methodology, Supervision, Writing–original draft, Writing–review and editing. YW: Conceptualization, Formal Analysis, Investigation, Methodology, Project administration, Resources, Supervision, Writing–original draft, Writing–review and editing.

Funding

The author(s) declare that financial support was received for the research, authorship, and/or publication of this article. This work was supported by the Lianyungang Traditional Chinese Medicine Science and Technology Development Program (Grant No. ZD202210).

Conflict of interest

The authors declare that the research was conducted in the absence of any commercial or financial relationships that could be construed as a potential conflict of interest.

Publisher's note

All claims expressed in this article are solely those of the authors and do not necessarily represent those of their affiliated organizations, or those of the publisher, the editors and the reviewers. Any product that may be evaluated in this article, or claim that may be made by its manufacturer, is not guaranteed or endorsed by the publisher.

References

- Arkaban, H., Barani, M., Akbarzadeh, M. R., Chauhan, N. P. S., Jadoun, S., Soltani, M. D., et al. (2022). Polyacrylic acid nanoplastics: antimicrobial, tissue engineering, and cancer theranostic applications. *Polymers-Basel* 14 (6), 1259. doi:10.3390/polym14061259
- Bakhshandeh, B., Zarrintaj, P., Oftadeh, M. O., Keramati, F., Fouladiha, H., Sohrabijahromi, S., et al. (2017). Tissue engineering: strategies, tissues, and biomaterials. *Biotechnol. Genet. Eng.* 33 (2), 144–172. doi:10.1080/02648725.2018.1430464
- Bhandari, M., Jeray, K. J., Petrisor, B. A., Devereaux, P. J., Heels-Ansdell, D., Schemitsch, E. H., et al. (2015). A trial of wound irrigation in the initial management of open fracture wounds. *New Engl. J. Med.* 373 (27), 2629–2641. doi:10.1056/NEJMoa1508502
- Budiatin, A. S., Gani, M., Samirah, A., Ardianto, C., Raharjanti, A. M., Septiani, I., et al. (2021). Bovine hydroxyapatite-based bone scaffold with gentamicin accelerates vascularization and remodeling of bone defect. *Int. J. Biomater.* 2021, 5560891–5560897. doi:10.1155/2021/5560891
- Cao, H., Duan, L. X., Zhang, Y., Cao, J., and Zhang, K. (2021). Current hydrogel advances in physicochemical and biological response-driven biomedical application diversity. *Signal. Transduct. Target* 6 (1), 426. doi:10.1038/s41392-021-00830-x
- Chee, E., and Brown, A. C. (2020). Biomimetic antimicrobial material strategies for combating antibiotic resistant bacteria. *Biomater. Sci-Uk* 8 (4), 1089–1100. doi:10.1039/c9bm01393h
- Cortés-Penfield, N. W., and Kulkarni, P. A. (2019). The history of antibiotic treatment of osteomyelitis. *Open. Forum. Infect. Dis.* 6 (5), 181. doi:10.1093/ofid/ofz181
- Cui, Y. T., Liu, H., Tian, Y. H., Fan, Y., Li, S. R., Wang, G., et al. (2022). Dual-functional composite scaffolds for inhibiting infection and promoting bone regeneration. *Mat. Today. Bio.* 16, 100409. doi:10.1016/j.mtbio.2022.100409
- Feng, Y. S., Zhu, S. J., Wang, L. G., Chang, L., Hou, Y. C., and Guan, S. K. (2018). Fabrication and characterization of biodegradable Mg-Zn-Y-Nd-Ag alloy: microstructure, mechanical properties, corrosion behavior and antibacterial activities. *Bioact. Mat.* 3 (3), 225–235. doi:10.1016/j.bioactmat.2018.02.002
- Habib, S., Rashid, F., Tahir, H., Liaqat, I., Latif, A. A., Naseem, S., et al. (2023). Antibacterial and cytotoxic effects of biosynthesized zinc oxide and titanium dioxide nanoparticles. *Microorganisms* 11 (6), 1363. doi:10.3390/microorganisms11061363
- Hu, X. H., Song, X. F., Xu, M. F., Wang, Y. H., Zhu, C. M., Yu, W. T., et al. (2023). A shape-memory poly(ϵ -caprolactone) hybridized TiO₂/poly(l-lactide) composite with antibacterial properties. *Int. J. Biol. Macromol.* 253, 126567. doi:10.1016/j.ijbiomac.2023.126567
- Jin, G. D., Cao, H. L., Qiao, Y. Q., Meng, F. H., Zhu, H. Q., and Liu, X. Y. (2014). Osteogenic activity and antibacterial effect of zinc ion implanted titanium. *Colloid. Surf. B* 117, 158–165. doi:10.1016/j.colsurfb.2014.02.025

- Jing, H. M., Yu, Z. M., and Li, L. (2008). Antibacterial properties and corrosion resistance of Cu and Ag/Cu porous materials. *J. Biomed. Mat. Res. A* 87 (1), 33–37. doi:10.1002/jbma.a.31688
- Kremers, H. M., Nwojo, M. E., Ransom, J. E., Wood-Wentz, C. M., Melton, L. J., and Huddleston, P. M. (2015). Trends in the epidemiology of osteomyelitis: A population-based study, 1969 to 2009. *J. Bone. Jt. Surg. Am.* 97 (10), 837–845. doi:10.2106/Jbjs.N.01350
- Li, B. B., Yang, T., Sun, R. X., and Ma, P. (2021). Biological and antibacterial properties of composite coatings on titanium surfaces modified by microarc oxidation and sol-gel processing. *Dent. Mat. J.* 40 (2), 455–463. doi:10.4012/dmj.2020-034
- Li, H., Guan, Z., Wei, L., Lu, J., Tan, Y., and Wei, Q. (2024). *In situ* co-deposition synthesis for collagen-Astragalus polysaccharide composite with intrafibrillar mineralization as potential biomimetic-bone repair materials. *Regen. Biomater.* 11, 070. doi:10.1093/rb/rbae070
- Li, P., Schille, C., Schweizer, E., Rupp, F., Heiss, A., Legner, C., et al. (2018). Mechanical characteristics, *in vitro* degradation, cytotoxicity, and antibacterial evaluation of Zn-4.0Ag alloy as a biodegradable material. *Int. J. Mol. Sci.* 19 (3), 755. doi:10.3390/ijms19030755
- Manjunatha, C., Rao, P. P., Bhardwaj, P., Raju, H., and Ranganath, D. (2021). New insight into the synthesis, morphological architectures and biomedical applications of elemental selenium nanostructures. *Biomed. Mat.* 16 (2), 022010. doi:10.1088/1748-605X/abc026
- Maqbool, M., Nawaz, Q., Rehman, M. A. U., Cresswell, M., Jackson, P., Hurlle, K., et al. (2021). Synthesis, characterization, antibacterial properties, and *in vitro* studies of selenium and strontium Co-substituted hydroxyapatite. *Int. J. Mol. Sci.* 22 (8), 4246. doi:10.3390/ijms22084246
- Molenda, M., and Kolmas, J. (2023). The role of zinc in bone tissue health and regeneration—a review. *Biol. Trace. Elem. Res.* 201 (12), 5640–5651. doi:10.1007/s12011-023-03631-1
- Naeem, A., Yu, C., and Wang, X. (2024). Highly swellable, cytocompatible and biodegradable guar gum-based hydrogel system for controlled release of bioactive components of licorice (*Glycyrrhiza glabra* L.): synthesis and evaluation. *Int. J. Biol. Macromol.* 273 (1), 132825. doi:10.1016/j.ijbiomac.2024.132825
- Nandi, S. K., Bandyopadhyay, S., Das, P., Samanta, I., Mukherjee, P., Roy, S., et al. (2016). Understanding osteomyelitis and its treatment through local drug delivery system. *Biotechnol. Adv.* 34 (8), 1305–1317. doi:10.1016/j.biotechadv.2016.09.005
- Nhu, V. T. T., Dat, N. D., Tam, L., and Phuong, N. H. (2022). Green synthesis of zinc oxide nanoparticles toward highly efficient photocatalysis and antibacterial application. *Beilstein. J. Nanotech.* 13, 1108–1119. doi:10.3762/bjnano.13.94
- Nishida, E., Miyaji, H., Shitomi, K., Sugaya, T., and Akasaka, T. (2021). Evaluation of antibacterial and cytocompatible properties of multiple-ion releasing zinc-fluoride glass nanoparticles. *Dent. Mat. J.* 40 (1), 157–164. doi:10.4012/dmj.2019-176
- Pineda, M. E. B., Forero, L. M. L., and Avila, C. A. S. (2022). Antibacterial activity of biosynthesized silver nanoparticles (AgNps) against *Pectobacterium carotovorum*. *Braz. J. Microbiol.* 53 (3), 1175–1186. doi:10.1007/s42770-022-00757-7
- Qin, B. Q., Dong, H. X., Tang, X. F., Liu, Y. J., Feng, G. Y., Wu, S. Z., et al. (2023). Antisense *yycF* and BMP-2 co-delivery gelatin methacryloyl and carboxymethyl chitosan hydrogel composite for infective bone defects regeneration. *Int. J. Biol. Macromol.* 253, 127233. doi:10.1016/j.ijbiomac.2023.127233
- Qiu, X., Li, S., Li, X., Xiao, Y., Li, S., Fen, Q., et al. (2022). Experimental study of β -TCP scaffold loaded with VAN/PLGA microspheres in the treatment of infectious bone defects. *Colloids. Surf. B. Biointerfaces.* 213, 112424. doi:10.1016/j.colsurfb.2022.112424
- Shen, H., and Hu, X. X. (2021). Growth factor loading on aliphatic polyester scaffolds. *Rsc. Adv.* 11 (12), 6735–6747. doi:10.1039/d0ra10232f
- Su, Y. C., Cockerill, I., Wang, Y. D., Qin, Y. X., Chang, L. Q., Zheng, Y. F., et al. (2019). Zinc-based biomaterials for regeneration and therapy. *Trends. Biotechnol.* 37 (4), 428–441. doi:10.1016/j.tibtech.2018.10.009
- Urish, K. L., and Cassat, J. E. (2020). *Staphylococcus aureus* osteomyelitis: bone, bugs, and surgery. *Infect. Immun.* 88 (7), e00932-19–e00919. doi:10.1128/IAI.00932-19
- Vergara-Llanos, D., Koning, T., Pavicic, M. F., Bello-Toledo, H., Díaz-Gómez, A., Jaramillo, A., et al. (2021). Antibacterial and cytotoxic evaluation of copper and zinc oxide nanoparticles as a potential disinfectant material of connections in implant provisional abutments: an *in-vitro* study. *Arch. Oral. Biol.* 122, 105031. doi:10.1016/j.archoralbio.2020.105031
- Wen, B., Dai, Y. G., Han, X., Huo, F. J., Xie, L., Yu, M., et al. (2023). Biomineralization-inspired mineralized hydrogel promotes the repair and regeneration of dentin/bone hard tissue. *Npj. Regen. Med.* 8 (1), 11. doi:10.1038/s41536-023-00286-3
- Xu, B., Zheng, P. B., Gao, F., Wang, W., Zhang, H. T., Zhang, X. R., et al. (2017). A mineralized high strength and tough hydrogel for skull bone regeneration. *Adv. Funct. Mat.* 27 (4), 1604327. doi:10.1002/adfm.201604327
- Xu, L. J., Ye, Q., Xie, J., Yang, J. J., Jiang, W. T., Yuan, H., et al. (2022). An injectable gellan gum-based hydrogel that inhibits *Staphylococcus aureus* for infected bone defect repair. *J. Mat. Chem. B* 10 (2), 282–292. doi:10.1039/d1tb02230j
- Xu, Y., Wen, W., and Wu, J. M. (2018). Titania nanowires functionalized polyester fabrics with enhanced photocatalytic and antibacterial performances. *J. Hazard. Mat.* 343, 285–297. doi:10.1016/j.jhazmat.2017.09.044
- Yang, X. T., Yu, Q. J., Gao, W., Tang, X. N., Yi, H. H., and Tang, X. L. (2022). The mechanism of metal-based antibacterial materials and the progress of food packaging applications: a review. *Ceram. Int.* 48 (23), 34148–34168. doi:10.1016/j.ceramint.2022.08.249
- You, C. G., Han, C. M., Wang, X. G., Zheng, Y. R., Li, Q. Y., Hu, X. L., et al. (2012). The progress of silver nanoparticles in the antibacterial mechanism, clinical application and cytotoxicity. *Mol. Biol. Rep.* 39 (9), 9193–9201. doi:10.1007/s11033-012-1792-8
- Yu, Y., Liu, K., Wen, Z., Liu, W., Zhang, L., and Su, J. (2020). Double-edged effects and mechanisms of Zn(2+) microenvironments on osteogenic activity of BMSCs: osteogenic differentiation or apoptosis. *Rsc. Adv.* 10 (25), 14915–14927. doi:10.1039/d0ra01465f
- Zhang, J. F., Cao, R. Y., Song, W. C., Liu, L., and Li, J. X. (2022). One-step method to prepare core-shell magnetic nanocomposite encapsulating silver nanoparticles with superior catalytic and antibacterial activity. *J. Colloid. Interf. Sci.* 607, 1730–1740. doi:10.1016/j.jcis.2021.09.053